23rd ABCM International Congress of Mechanical Engineering
December 6-11, 2015, Rio de Janeiro, RJ, Brazil

INVERSE DYNAMICS OF A NOVEL 9-DOF HYBRID MANIPULATOR USING KANE'S METHOD

Paulo Victor Gomes dos Santos
Max Suell Dutra
Universidade Federal do Rio de Janeiro - Ilha do Fundão, Rio de Janeiro, Brazil
pvg.santos@mecanica.coppe.ufrj.br max@mecanica.coppe.ufrj.br

Abstract. *Nowadays the offshore cargo transfer is being treated as a promising technology. The biggest challenge in offshore cargo transfer is to control and stabilize the load. However, to test control strategies in a real scenario is dangerous. Thus, it is necessary the development of mechanisms that simulates the behavior of cranes that are fixed on floating platforms like vessels and offshore platforms. This paper presents the equations of motion for a hybrid parallel-serial manipulator. This manipulator is composed by a modified SCARA robot coupled to a Stewart-Gough platform, which is designed to simulate a crane operating on a floating platform. This hybrid robot is considered as a nine degrees of freedom system composed of seventeen bodies. The equations of motion are obtained using the Kane's method. The inverse dynamics equations are derived and simulated. This work will allow the design of a serial manipulator to be attached to an already built Stewart-Gough platform.*

Keywords: *Inverse Dynamics, Hybrid Manipulator, Kane formulation*

1. INTRODUCTION

Since remote times, the sea shipping trade has a huge impact on humankind activities. In face of this importance, new technologies and methods that promote any advance in sectors that allow technological or logistics advantages arouse interest around the world. A new technology that has been treated as a promising one is the offshore cargo transfer operation. This technology aims the transfer of containers between vessels or between a vessel and an offshore platform. The biggest challenge in offshore cargo transfer is to control and stabilize the load, in a manner that it can be allocated in another ship smoothly. However, to develop and test control strategies in a real scenario is dangerous. Thus, it is necessary the development of mechanisms that simulates the behavior of cranes that are fixed on floating platforms, like vessels, and offshore platforms. In this paper it is proposed a new hybrid manipulator designed to simulate a novel crane to be used in offshore cargo transfer operations.

The robot manipulators can be classified into three types: serial, parallel and hybrid. Siciliano *et al.* (2009) defines the serial robot as a mechanism composed by an open kinematic chain. The parallel robot is defined by Merlet (2006) as a robot that is made up of an end-effector with n degrees of freedom and a fixed base, linked together by at least two independent kinematic chains, whose actuation takes place through n simple actuators. According to Tanev (2000), a hybrid type manipulation system is a combination of closed-chain and open-chain mechanisms or it is a sequence of parallel mechanisms. Hybrid manipulators conjugate the main advantages of serial and parallel manipulators, they have a considerable workspace in addition to a rigid architecture (Alvarado, 2005).

Among the serial robots, the SCARA manipulator has one of the best ratio of the load capacity/robot mass (Merlet, 2006). Based on this, it was proposed a new architecture of a serial robot based on the SCARA manipulator to be used in the offshore cargo transfer operations. Moreover, a Stewart-Gough platform is a type of parallel manipulator that can simulate the 6-DOF of a floating body. By the coupling of this serial manipulator with the parallel manipulator a new type of hybrid robot is proposed, Fig 1.

2. KANE'S METHOD

Kane and Levinson (1985) have proposed a general method for obtaining the equations of motion of multi-bodies holonimic or nonholonomic systems. According to Kane and Levinson (1985), the expressions of the angular velocities of rigid bodies and the linear velocities of the points of a system S , in which the configuration in an inertial frame R_1 can be defined by n generalized coordinates $(q_1, ..., q_n)$ can be written in a particularly advantageous way with the introduction of n quantities $(u_1, ..., u_n)$ called generalized speeds for S in R_1. These quantities are defined as Eq. (1).

$$u_r = \sum_{s=1}^{n} Y_{rs}\dot{q}_s + Z_r \quad r = 1, 2, ..., n \tag{1}$$

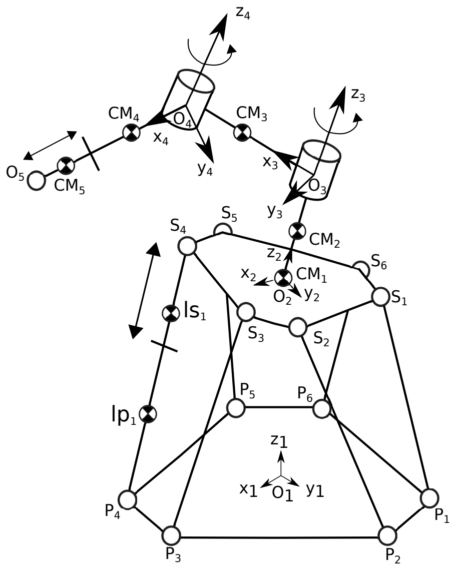

Figure 1. Hybrid robot for offshore cargo transfer simulation

Where Y_{rs} and Z_r are functions of the time t. These functions need to be chosen in a way that Eq. (1) has only one solution for $\dot{q_1}, ...\dot{q_n}$. Using this equation, the linear velocities $\boldsymbol{v}$ and the angular velocities $\boldsymbol{\omega}$ can be written as:

$$\boldsymbol{v} = \sum_{r=1}^{n} \boldsymbol{v}_r u_r + \boldsymbol{v}_t \tag{2}$$

$$\boldsymbol{\omega} = \sum_{r=1}^{n} \boldsymbol{\omega}_r u_r + \boldsymbol{\omega}_t \tag{3}$$

Where $\boldsymbol{v}_r$, $\boldsymbol{\omega}_r$, $\boldsymbol{v}_t$, $\boldsymbol{\omega}_t$ are functions of $q_1, ..., q_n$, and the time t. The vector $\boldsymbol{v}_r$ is called partial velocity and $\boldsymbol{\omega}_r$ is called partial angular velocity. Using these terms,Kane and Levinson (1985) defined the generalized active forces as:

$$F_r = \sum_{i=1}^{\nu} \boldsymbol{v}_r^{P_i} \cdot \boldsymbol{R}_i + {}^{R_1}\boldsymbol{\omega}_r^{R_k} \cdot \boldsymbol{T}_i \quad r = 1, 2, ..., n \tag{4}$$

Where ν is the number of bodies comprising S, R_k is the reference frame fixed in the i^{th} body of S, P_i is a typical particle of the i^{th} body of S, $\boldsymbol{v}_r^{P_i}$ and ${}^{R_1}\boldsymbol{\omega}_r^{R_k}$ are, respectively, the partial velocity and the partial angular velocity of P_i in R_1, and $\boldsymbol{R_i}$ and $\boldsymbol{T_i}$ are, respectively, the resulting of all forces and torques acting on P_i. In a similar way, Kane and Levinson (1985) defined the generalized inertial forces as:

$$F_r^* = \sum_{i=1}^{\nu} \boldsymbol{v}_r^{P_i} \cdot (-m_i \boldsymbol{a_i}) - {}^{R_1}\boldsymbol{\omega}_r^{R_k} \cdot (\boldsymbol{I}_{m_i} \cdot {}^{R_1}\boldsymbol{\alpha}^{R_k} + {}^{R_1}\boldsymbol{\omega}^{R_k} \times \boldsymbol{I}_{m_i} \cdot {}^{R_1}\boldsymbol{\omega}^{R_k}) \quad r = 1, 2, ..., n \tag{5}$$

Where m_i, $\boldsymbol{a_i}$, and $\boldsymbol{I}_{m_i}$ are, respectively, the mass, the acceleration and the inertia of the i^{th} body, and ${}^{R_1}\boldsymbol{\omega}^{R_k}$ and ${}^{R_1}\boldsymbol{\alpha}^{R_k}$ are, respectively, the angular velocity and the angular acceleration of the frame R_k in R_1. The equations of motions are obtained by the sum of Eq. (4) and Eq. (5). According to Liu *et al.* (2005), the form of the equations is quite simple, and calculating Kane equations only engages in additions, subtractions, and multiplications, thereby it is significantly convenient to construct and solve the dynamic equations for complex systems.

3. DYNAMIC MODELING OF 9-DEGREE-OF-FREEDOM HYBRID ROBOT

In this section, the dynamic equations of the hybrid robot are obtained. In order to make the analysis easier to understand, it will be divided in two parts, the serial and the parallel. Then the equations derived in each part will be coupled to obtain the dynamic equations of the hybrid robot.

3.1 Dynamic Modeling of the Parallel Robot

As stated by Meng *et al.* (2010), in the dynamic modeling of the Stewart-Gough platform when the inertia of the load was not much larger than that of the actuators, the effect of actuators inertia is no longer negligible; thus, the parallel robot is modeled as a system compound by thirteen bodies in a closed kinematic chain. The dynamic equations of this system using Kane's formulation were obtained by Yang *et al.* (2012), Liu *et al.* (2000), Meng *et al.* (2010), and Wu *et al.* (2012). However, in this paper it will be used a new approach that combines the Kane's method with the exponential formulation to represent rotations. According to Murray *et al.* (1994), a rotation of a rigid body can be represented as:

$$R(\boldsymbol{\omega}, \theta) = e^{\widehat{\omega}\theta} = e^{\widehat{\Omega}t} \tag{6}$$

Where $\boldsymbol{\omega} \in \mathbb{R}^3$ is a unit vector which specifies the direction of rotation, $\theta \in \mathbb{R}$ is the angle of rotation in radians, and $\boldsymbol{\Omega} \in \mathbb{R}^3$ is the angular velocity of the body. The operator $\widehat{}$ converts a 3×1 vector into a 3×3 screw matrix.

The length of each leg is obtained by Eq. (7):

$$\boldsymbol{l_i} = \boldsymbol{p^{O_1/O_2}} \cdot \boldsymbol{n_1 n_1} + e^{\widehat{\Omega}^{R_2}t}\boldsymbol{p^{O_2/S_i}} \cdot \boldsymbol{n_2 n_1} - \boldsymbol{p^{O_1/P_i}} \cdot \boldsymbol{n_1 n_1} \quad i = 1, 2, ..., 6 \tag{7}$$

Where $\boldsymbol{l_i}$ is the position vector of point S_i to point P_i, $\boldsymbol{p^{O_1/O_2}}$ is the position vector of the point O_2 to point O_1, $\boldsymbol{p^{O_2/S_i}}$ is the position vector of point S_i to O_2, $\boldsymbol{p^{O_1/P_i}}$ is the position vector of point P_i to O_1, R_2 is a reference frame fixed at the center of mass of the movable platform, $\boldsymbol{\Omega}^{R_2}$ is the angular velocity of the frame R_2 to the inertial frame R_1, $\boldsymbol{n_1}$ is a orthonormal vector basis that compound the reference frame R_1, and, similarly, $\boldsymbol{n_2}$ compound R_2. These points can be seen in Fig. 1.

Equation (7) is differentiated in R_1:

$$\dot{\boldsymbol{l_i}} = \frac{{}^{R_1}d\boldsymbol{l_i}}{dt} = \boldsymbol{v}^{cm_1} + \boldsymbol{\Omega}^{R2} \times e^{\widehat{\Omega}^{R_2}t}\boldsymbol{p^{O_2/Si}} \cdot \boldsymbol{n_2 n_1} \tag{8}$$

The velocity of the center of mass of the movable platform $\boldsymbol{v}^{cm_1}$ is:

$$\boldsymbol{v}^{cm_1} = \dot{q}_1\boldsymbol{x_1} + \dot{q}_2\boldsymbol{y_1} + \dot{q}_3\boldsymbol{z_1} \tag{9}$$

To describe the movement of the movable platform six generalized coordinates are used, which q_1, q_2, and q_3 are the translation movement at the $\boldsymbol{x_1}$, $\boldsymbol{y_1}$, $\boldsymbol{z_1}$ axis, respectively. Moreover, q_4, q_5, and q_6 represent the rotation movement at these axis, respectively. The vectors $\boldsymbol{x_1}$, $\boldsymbol{y_1}$ and $\boldsymbol{z_1}$ are the orthonormal vector basis of R_1. An unit vector $\boldsymbol{ul_i}$ that has the same direction of $\boldsymbol{l_i}$ is created. Considering the length of the i^{th} leg as l_i, Eq. (7) can be written as:

$$\boldsymbol{l_i} = l_i\boldsymbol{ul_i} \tag{10}$$

Equation (11) is derived by the differentiation of Eq. (10) in R_1:

$$\dot{\boldsymbol{l_i}} = \dot{l_i}\, \boldsymbol{ul_i} + \boldsymbol{\Omega}^{R_{l_i}} \times l_i\boldsymbol{ul_i} \tag{11}$$

Cross-producting both sides of Eq. (11) with $\boldsymbol{ul_i}$ and equating to Eq. (8), the angular velocity of the i^{th} leg in R_1 can be derived:

$$\boldsymbol{\Omega}^{R_{l_i}} = \frac{\boldsymbol{ul_i} \times \left(\boldsymbol{v}^{cm_1} + \boldsymbol{\Omega}^{R_2} \times e^{\widehat{\Omega}^{R_2}t}\boldsymbol{p}^{O_2/S_i}\right)}{l_i} \tag{12}$$

Where R_{l_i} is a reference frame fixed at the i^{th} leg.

The angular acceleration of the i^{th} leg $\boldsymbol{\alpha}^{R_{l_i}}$ can be obtained by the differentiation of the Eq. (12):

$$\begin{aligned} \boldsymbol{\alpha}^{R_{l_i}} = \frac{{}^{R_1}d\boldsymbol{\Omega}^{R_{l_i}}}{dt} = \boldsymbol{\Omega}^{R_{l_i}} \times \left(\frac{\boldsymbol{ul_i}}{l_i} \times \left(\boldsymbol{v}^{cm_1} + \boldsymbol{\Omega}^{R_2} \times e^{\widehat{\Omega}^{R_2}t}\boldsymbol{p}^{O_2/S_i}\right)\right) + \\ + \frac{\boldsymbol{ul_i}}{l_i} \times \left(\boldsymbol{a}^{cm_1} + \boldsymbol{\alpha}^{R_2} \times e^{\widehat{\Omega}^{R_2}t}\boldsymbol{p}^{O_2/S_i} + \boldsymbol{\Omega}^{R_2} \times \boldsymbol{\Omega}^{R_2} \times e^{\widehat{\Omega}^{R_2}t}\boldsymbol{p}^{O_2/S_i}\right) \end{aligned} \tag{13}$$

Where $\boldsymbol{a}^{cm_1}$ is the temporal differential of $\boldsymbol{v}^{cm_1}$ in R_1. Each leg is compound by two links. The position of the center of mass of the bottom link $\boldsymbol{p}^{P_i/lp_i}$ is:

$$\boldsymbol{p}^{P_i/lp_i} = \frac{lc}{2}\boldsymbol{ul_i} \tag{14}$$

Where lc is the length of the bottom link. The position of the center of mass of the upper link $\boldsymbol{p}^{P_i/ls_i}$ is:

$$\boldsymbol{p}^{P_i/ls_i} = \frac{(l_i + lc)}{2}\boldsymbol{ul_i} \tag{15}$$

Differentiating the Eq. (14) and Eq. (15) twice, the accelerations of the center of mass of upper and bottom links, respectively, $\boldsymbol{a}^{ls_i}$ and $\boldsymbol{a}^{lp_i}$ can be derived:

$$\boldsymbol{a}^{ls_i} = \frac{1}{2}(\ddot{l}_i\ \boldsymbol{ul_i} + \boldsymbol{\Omega}^{R_{l_i}} \times \boldsymbol{\Omega}^{R_{l_i}} \times (l_i + lc)\boldsymbol{ul_i} + 2\boldsymbol{\Omega}^{R_{l_i}} \times \dot{l}_i\ \boldsymbol{ul_i} + \boldsymbol{\alpha}^{R_{l_i}} \times (l_i + lc)\boldsymbol{ul_i}) \tag{16}$$

$$\boldsymbol{a}^{lp_i} = \frac{lc}{2}\left(\boldsymbol{\Omega}^{R_{l_i}} \times \boldsymbol{\Omega}^{R_{l_i}} \times \boldsymbol{ul_i} + \boldsymbol{\alpha}^{R_{l_i}} \times \boldsymbol{ul_i}\right) \tag{17}$$

As stated by Kane and Levinson (1985), if the generalized speeds are chosen as Eq. (18), the partial velocities can be derived as shown by Eq. (19)

$$u_r = \frac{dq_r}{dt} \tag{18}$$

$$\boldsymbol{v}_r = \frac{\partial \boldsymbol{p}}{\partial q_r} \tag{19}$$

The partial velocities of the center of mass of the movable platform, center of mass of the upper link, and center of mass of the bottom link, respectively, $\boldsymbol{v}_r^{cm_1}$, $\boldsymbol{v}_r^{ls_i}$, and $\boldsymbol{v}_r^{lp_i}$ are derived:

$$\boldsymbol{v}_r^{cm_1} = \frac{\partial \boldsymbol{p}^{O_1/O_2}}{\partial q_r} \quad r = 1, 2, 3, ..., 6 \tag{20}$$

$$\boldsymbol{v}_r^{ls_i} = \frac{\partial \boldsymbol{p}^{P_i/Ls_i}}{\partial q_r} = \frac{(l_i + lc)}{2}\boldsymbol{\omega}_r^{Rl_i} \times e^{\sum_{r=1}^{6} \widehat{\omega}_r^{Rl_i} q_r}\boldsymbol{n_1} + \frac{1}{2}\frac{\partial \boldsymbol{l_i}}{\partial q_r} \tag{21}$$

$$\boldsymbol{v}_r^{lp_i} = \boldsymbol{\omega}_r^{Rl_i} \times e^{\sum_{r=1}^{6} \widehat{\omega}_r^{Rl_i} q_r} \cdot \frac{lc}{2}\boldsymbol{n_1} \tag{22}$$

Where $\boldsymbol{\omega}_r^{Rl_i}$ is the partial angular velocity of $\boldsymbol{\Omega}^{R_{l_i}}$.

$$\boldsymbol{\omega}_r^{Rl_i} = \frac{\boldsymbol{ul_i}}{l_i} \times \left(\boldsymbol{v}_r^{cm_1} + \boldsymbol{\omega}_r^{R_2} \times e^{\widehat{\Omega}^{R_2} t}\boldsymbol{p}^{O_2/S_1}\right) \tag{23}$$

And $\boldsymbol{\omega}_r^{R_2}$ is the partial angular velocity of movable platform:

$$\boldsymbol{\omega}_r^{R_2} = \frac{\partial \boldsymbol{\Omega}^{\boldsymbol{R_2}}}{\partial \dot{q}_r} \quad r = 1, 2, ..., 6 \tag{24}$$

The generalized active forces and the generalized inertia forces of the Stewart-Gough platform are derived:

$$F_r = m_1\boldsymbol{g}\cdot\boldsymbol{v}_r^{cm_1} + \sum_{i=1}^{6}(F_{l_i}(\boldsymbol{p}^{O_2/S_i}\times\boldsymbol{ul_i})\cdot\boldsymbol{\omega}_r^{R_2} + F_{l_i}\boldsymbol{ul_i}\cdot\boldsymbol{v}_r^{cm_1} + m_{lp_i}\boldsymbol{g}\cdot\boldsymbol{v}_r^{lp_i} + m_{ls_i}\boldsymbol{g}\cdot\boldsymbol{v}_r^{ls_i}) \qquad r = 1,2,...,6 \tag{25}$$

$$\begin{aligned}F_r^* = -(m_1\boldsymbol{a}^{cm_1}\cdot\boldsymbol{v}_r^{cm_1} + \left(\boldsymbol{I}_{m_1}\cdot\boldsymbol{\alpha}^{R_2} + \boldsymbol{\Omega}^{R_2}\times\boldsymbol{I}_{m_1}\boldsymbol{\Omega}^{R_2}\right)\cdot\boldsymbol{\omega}_r^{R_2} + \sum_{i=1}^{6}(m_{lp_i}\boldsymbol{a}^{lp_i}\cdot\boldsymbol{v}_r^{lp_i} + m_{ls_i}\boldsymbol{a}^{ls_i}\cdot\boldsymbol{v}_r^{ls_i} +\\ + \left((\boldsymbol{I}_{lp_i}+\boldsymbol{I}_{ls_i})\cdot\boldsymbol{\alpha}^{Rl_i} + \boldsymbol{\Omega}^{Rl_i}\times(\boldsymbol{I}_{ls_i}+\boldsymbol{I}_{lp_i})\,\boldsymbol{\Omega}^{Rl_i}\right)\cdot\boldsymbol{\omega}_r^{Rl_i}))\\ r = 1,2,...,6\end{aligned} \tag{26}$$

Where $\boldsymbol{g}$ is the gravity force, m_1 and $\boldsymbol{I}_{m_1}$ are, respectively the mass and the tensor of inertia of the movable platform. m_{ls_i} and $\boldsymbol{I}_{ls_i}$ are, respectively the mass and the tensor of inertia of the upper links. And m_{lp_i} and $\boldsymbol{I}_{lp_i}$ are, respectively the mass and the tensor of inertia of the bottom links. F_{l_i} is the force that the i^{th} linear actuator apply at the movable platform.

3.2 Dynamic Modeling of the Serial Robot

In this subsection, a novel method to derive the dynamic equations of a general serial robot is presented. This method combines the Kane's method with the exponential formulation to describe rotations. A general robot is presented in Fig 2.

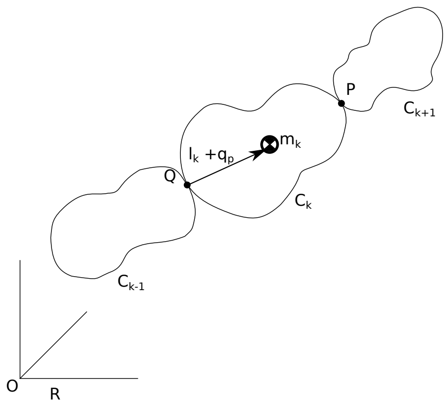

Figure 2. General serial robot

Equation (27) shows the position vector of the center of mass of the k^{th} body. Where the point O is the origin of the system, the point m_k is the center of mass of the k^{th} body, $\boldsymbol{\Omega^{R_k}}$ is the angular velocity of the k^{th} body to the inertial frame R_1, q_p is a generalized coordinate associated to a translation movement.

$$\boldsymbol{p}^{O/m_k} = \boldsymbol{p}^{O/Q}\cdot\boldsymbol{n}_1\boldsymbol{n}_1 + e^{\widehat{\Omega}^{R_k}t}(l_k+q_p)\boldsymbol{n}_1 \tag{27}$$

The angular velocity Ω^{R_k} can be written as:

$$\boldsymbol{\Omega}^{R_k} = \boldsymbol{\omega}_1^{R_k}\dot{q_1} + \boldsymbol{\omega}_2^{R_k}\dot{q_2} + ... + \boldsymbol{\omega}_n^{R_k}\dot{q_n} \tag{28}$$

Where q_1, q_2, ..., q_n are the generalized coordinates associated to the rotation movements of the k^{th} body. The axis $\boldsymbol{\omega}_1^{R_k}$, ..., $\boldsymbol{\omega}_n^{R_k}$ are the rotation axis of the revolution joints. If the generalized speeds are chosen as Eq. (18), these axis are also the partial angular velocities.

Differentiating the Eq. (27) twice, the acceleration of the center of mass of the k^{th} body is obtained:

$$\begin{aligned}{}^{R_1}\boldsymbol{a}^{cm_k} = {}^{R_1}\boldsymbol{a}^Q + \boldsymbol{\Omega}^{R_k}\times\boldsymbol{\Omega}^{R_k}\times e^{\widehat{\Omega}^{R_k}t}(l_k+q_p)\boldsymbol{n}_1 + \boldsymbol{\alpha}\times e^{\widehat{\Omega}^{R_k}t}(l_k+q_p)\boldsymbol{n}_1 +\\ 2\dot{q}_p\boldsymbol{\Omega}^{R_k}\times e^{\widehat{\Omega}^{R_k}t}\boldsymbol{n}_1 + \ddot{q}_p e^{\widehat{\Omega}^{R_k}t}\boldsymbol{n}_1\end{aligned} \tag{29}$$

The partial velocities of the center of mass of the k^{th} body can be obtained by the partial differentiate of the Eq. (27):

$$\boldsymbol{v}_r^{cm_k} = \boldsymbol{v}_r^{Q} + \boldsymbol{\omega}_r^{R_k} \times \boldsymbol{p}^{Q/m_k} + \frac{\partial q_k}{\partial q_r} e^{\sum_{s=1}^{n} \widehat{\omega}_s^{R_k} q_s} \boldsymbol{n_1} \quad r = 1, 2, ..., k, ..., n \tag{30}$$

Where $\boldsymbol{p}^{Q/m_k}$ is the position vector of the center of mass of the k^{th} body to the point Q and n is the number of degrees of freedom of the serial robot.

Thus, the equations of motion of a general serial robot compound by S links are derived:

$$\sum_{i=1}^{S} \boldsymbol{v}_r^{cm_i} \cdot (m_i \boldsymbol{a}^{cm_i}) + \boldsymbol{\omega}_r^{R_i} \cdot (\boldsymbol{I}_{mi} \cdot \boldsymbol{\alpha}^{R_i} + \boldsymbol{\Omega}^{R_i} \times \boldsymbol{I}_{m_i} \cdot \boldsymbol{\Omega}^{R_i}) = \sum_{i=1}^{S} \boldsymbol{v}_r^{cm_i} \cdot \boldsymbol{F_i} + \boldsymbol{\omega}_r^{R_i} \cdot \boldsymbol{T_i} \quad r = 1, 2, ..., n \tag{31}$$

Where m_i and $\boldsymbol{I}_{m_i}$ are, respectively, the mass and the tensor of inertia of the i^{th} link. $\boldsymbol{T_i}$ is the active torque applied at the i^{th} rotation joint and $\boldsymbol{F_i}$ is the active force applied at the i^{th} prismatic joint.

Applying this method to the modified SCARA robot shown in Fig. 1 coupled to the parallel robot, the generalized active forces and the generalized inertia forces, respectively, of this serial robot can be derived.

$$\begin{gathered} F_r = m_2 \boldsymbol{g} \cdot \boldsymbol{v}_r^{cm_2} + m_3 \boldsymbol{g} \cdot \boldsymbol{v}_r^{cm_3} + m_4 \boldsymbol{g} \cdot \boldsymbol{v}_r^{cm_4} + m_5 \boldsymbol{g} \cdot \boldsymbol{v}_r^{cm_5} + \\ \left(\boldsymbol{\omega}_r^{R_3} - \boldsymbol{\omega}_r^{R_2}\right) \cdot \boldsymbol{T_1} + \left(\boldsymbol{\omega}_r^{R_4} - \boldsymbol{\omega}_r^{R_4}\right) \cdot \boldsymbol{T_2} + \left(\boldsymbol{v}_r^{cm_4} - \boldsymbol{v}_r^{cm_5}\right) \cdot \boldsymbol{F_s} \qquad r = 1, 2, ..., 9 \end{gathered} \tag{32}$$

$$\begin{gathered} F_r^* = -(m_2 \boldsymbol{a}^{cm_2} \cdot \boldsymbol{v}_r^{cm_2} + m_3 \boldsymbol{a}^{cm_3} \cdot \boldsymbol{v}_r^{cm_3} + m_4 \boldsymbol{a}^{cm_4} \cdot \boldsymbol{v}_r^{cm_4} + m_5 \boldsymbol{a}^{cm_5} \cdot \boldsymbol{v}_r^{cm_5} + \\ \left(\boldsymbol{I}_{m_2} \cdot \boldsymbol{\alpha}^{R_2} + \boldsymbol{\Omega}^{R_2} \times \boldsymbol{I}_{m_2} \boldsymbol{\Omega}^{R_2}\right) \cdot \boldsymbol{\omega}_r^{R_2} + \left(\boldsymbol{I}_{m_3} \cdot \boldsymbol{\alpha}^{R_3} + \boldsymbol{\Omega}^{R_3} \times \boldsymbol{I}_{m_3} \cdot \boldsymbol{\Omega}^{R_3}\right) \cdot \boldsymbol{\omega}_r^{R_3} + \\ \left((\boldsymbol{I}_{m_4} + \boldsymbol{I}_{m_5}) \cdot \boldsymbol{\alpha}^{R_4} + \boldsymbol{\Omega}^{R_4} \times (\boldsymbol{I}_{m_4} + \boldsymbol{I}_{m_5}) \boldsymbol{\Omega}^{R_4}\right) \cdot \boldsymbol{\omega}_r^{R_4}) \qquad r = 1, 2, ..., 9 \end{gathered} \tag{33}$$

Where q_7, q_8, and q_9 are, respectively, the angle of the first and second rotation joints and the displacement of the prismatic joint of the serial robot. $\boldsymbol{\Omega}^{R_3}$ and $\boldsymbol{\Omega}^{R_4}$ are, respectively, the reference frames fixed at the second and third links of the serial robot. The subscript 2,3,4, and 5 refers to the first, second, third and fourth links of the serial robot, because the subscript 1 was used to represent the movable platform. $\boldsymbol{T_1}$ and $\boldsymbol{T_2}$ are the active torques at the first and second rotation joints and $\boldsymbol{F_s}$ is the active force acting at the prismatic joint of the serial robot.

3.3 Dynamic Modeling of the Hybrid Robot

The generalized active forces of the hybrid robot can be derived by adding the equation 25 with equation 32:

$$\begin{aligned} F_r = {} & m_1 \boldsymbol{g} \cdot \boldsymbol{v}_r^{cm_1} + m_2 \boldsymbol{g} \cdot \boldsymbol{v}_r^{cm_2} + m_3 \boldsymbol{g} \cdot \boldsymbol{v}_r^{cm_3} + m_4 \boldsymbol{g} \cdot \boldsymbol{v}_r^{cm_4} + m_5 \boldsymbol{g} \cdot \boldsymbol{v}_r^{cm_5} + \left(\boldsymbol{\omega}_r^{R_3} - \boldsymbol{\omega}_r^{R_2}\right) \cdot \boldsymbol{T_1} + \\ & \left(\boldsymbol{\omega}_r^{R_4} - \boldsymbol{\omega}_r^{R_3}\right) \cdot \boldsymbol{T_2} + \left(\boldsymbol{v}_r^{cm_4} - \boldsymbol{v}_r^{cm_5}\right) \cdot \boldsymbol{F_s} + \sum_{i=1}^{6} (F_{l_i} (\boldsymbol{p}^{O_2/S_i} \times \boldsymbol{ul_i}) \cdot \boldsymbol{\omega}_r^{R_2} + F_{l_i} \boldsymbol{ul_i} \cdot \boldsymbol{v}_r^{cm_1} + \\ & m_{lp_i} \boldsymbol{g} \cdot \boldsymbol{v}_r^{lp_i} + m_{ls_i} \boldsymbol{g} \cdot \boldsymbol{v}_r^{ls_i}) \qquad r = 1, 2, ..., 9 \end{aligned} \tag{34}$$

Moreover the generalized inertia forces of the hybrid robot can be derived by adding the Eq.(26) with Eq.(33):

$$\begin{aligned} F_r^* = {} & -(m_1 \boldsymbol{a}^{cm_1} \cdot \boldsymbol{v}_r^{cm_1} + m_2 \boldsymbol{a}^{cm_2} \cdot \boldsymbol{v}_r^{cm_2} + m_3 \boldsymbol{a}^{cm_3} \cdot \boldsymbol{v}_r^{cm_3} + m_4 \boldsymbol{a}^{cm_4} \cdot \boldsymbol{v}_r^{cm_4} + m_5 \boldsymbol{a}^{cm_5} \cdot \boldsymbol{v}_r^{cm_5} + \\ & \left((\boldsymbol{I}_{m_1} + \boldsymbol{I}_{m_2}) \cdot \boldsymbol{\alpha}^{R_2} + \boldsymbol{\Omega}^{R_2} \times (\boldsymbol{I}_{m_1} + \boldsymbol{I}_{m_2}) \boldsymbol{\Omega}^{R_2}\right) \cdot \boldsymbol{\omega}_r^{R_2} + \left(\boldsymbol{I}_{m_3} \cdot \boldsymbol{\alpha}^{R_3} + \boldsymbol{\Omega}^{R_3} \times \boldsymbol{I}_{m_3} \cdot \boldsymbol{\Omega}^{R_3}\right) \cdot \boldsymbol{\omega}_r^{R_3} + \\ & \left((\boldsymbol{I}_{m_4} + \boldsymbol{I}_{m_5}) \cdot \boldsymbol{\alpha}^{R_4} + \boldsymbol{\Omega}^{R_4} \times (\boldsymbol{I}_{m_4} + \boldsymbol{I}_{m_5}) \boldsymbol{\Omega}^{R_4}\right) \cdot \boldsymbol{\omega}_r^{R_4} + \sum_{i=1}^{6} (m_{lp_i} \boldsymbol{a}^{lp_i} \cdot \boldsymbol{v}_r^{lp_i} + m_{ls_i} \boldsymbol{a}^{ls_i} \cdot \boldsymbol{v}_r^{ls_i} + \\ & \left((\boldsymbol{I}_{lp_i} + \boldsymbol{I}_{ls_i}) \cdot \boldsymbol{\alpha}^{Rl_i} + \boldsymbol{\Omega}^{Rl_i} \times (\boldsymbol{I}_{ls_i} + \boldsymbol{I}_{lp_i}) \boldsymbol{\Omega}^{Rl_i}\right) \cdot \boldsymbol{\omega}_r^{Rl_i})) \qquad r = 1, 2, ..., 9 \end{aligned} \tag{35}$$

Thus, the dynamics equations of motion are derived adding Eq.(34) with Eq.(35):

$$F_r + F_r^* = 0 \quad r = 1, 2, ..., 9 \tag{36}$$

4. SIMULATION OF THE INVERSE DYNAMICS

The inverse dynamics problem consists of determining the joint forces and torques which are needed to generate the motion specified by the joint accelerations $\ddot{q}(t)$, velocities $\dot{q}(t)$ and positions $q(t)$ (Siciliano *et al.*, 2009). Equation (36) can be turned into a matrix equation:

$$\boldsymbol{AX} = \boldsymbol{B} \tag{37}$$

Where the lines of matrix $\boldsymbol{A}$ are:

$$\begin{aligned}\boldsymbol{A}_r = [&(\boldsymbol{\omega}_r^{R_3} - \boldsymbol{\omega}_r^{R_2}) \cdot \boldsymbol{z_3},\ (\boldsymbol{\omega}_r^{R_4} - \boldsymbol{\omega}_r^{R_3}) \cdot \boldsymbol{z_4}, (\boldsymbol{v}_r^{cm_4} - \boldsymbol{v}_r^{cm_5}) \cdot \boldsymbol{x_4},\ \boldsymbol{ul_1} \cdot \boldsymbol{v}_r^{cm_1} + (\boldsymbol{p}^{O_2/S_1} \times \boldsymbol{ul_1}) \cdot \boldsymbol{\omega}_r^{R_2},\\ &\boldsymbol{ul_2} \cdot \boldsymbol{v}_r^{cm_1} + (\boldsymbol{p}^{O_2/S_2} \times \boldsymbol{ul_2}) \cdot \boldsymbol{\omega}_r^{R_2},\ \dots,\ \boldsymbol{ul_6} \cdot \boldsymbol{v}_r^{cm_1} + (\boldsymbol{p}^{O_2/S_6} \times \boldsymbol{ul_6}) \cdot \boldsymbol{\omega}_r^{R_2}] \quad r = 1,2,3,\dots,9\end{aligned} \tag{38}$$

The elements of vector $\boldsymbol{B}$ are:

$$\begin{aligned}\boldsymbol{B}_r = {}& m_1 \boldsymbol{a}^{cm_1} \cdot \boldsymbol{v}_r^{cm_1} + m_2 \boldsymbol{a}^{cm_2} \cdot \boldsymbol{v}_r^{cm_2} + m_3 \boldsymbol{a}^{cm_3} \cdot \boldsymbol{v}_r^{cm_3} + m_4 \boldsymbol{a}^{cm_4} \cdot \boldsymbol{v}_r^{cm_4} + m_5 \boldsymbol{a}^{cm_5} \cdot \boldsymbol{v}_r^{cm_5} +\\ &\Big((\boldsymbol{I}_{m_1} + \boldsymbol{I}_{m_2}) \cdot \boldsymbol{\alpha}^{R_2} + \boldsymbol{\Omega}^{R_2} \times (\boldsymbol{I}_{m_1} + \boldsymbol{I}_{m_2}) \boldsymbol{\Omega}^{R_2}\Big) \cdot \boldsymbol{\omega}_r^{R_2} + \Big(\boldsymbol{I}_{m_3} \cdot \boldsymbol{\alpha}^{R_3} + \boldsymbol{\Omega}^{R_3} \times \boldsymbol{I}_{m_3} \cdot \boldsymbol{\Omega}^{R_3}\Big) \cdot \boldsymbol{\omega}_r^{R_3} +\\ &\Big((\boldsymbol{I}_{m_4} + \boldsymbol{I}_{m_5}) \cdot \boldsymbol{\alpha}^{R_4} + \boldsymbol{\Omega}^{R_4} \times (\boldsymbol{I}_{m_4} + \boldsymbol{I}_{m_5}) \boldsymbol{\Omega}^{R_4}\Big) \cdot \boldsymbol{\omega}_r^{R_4} + \sum_{i=1}^{6} (m_{lp_i} \boldsymbol{a}^{lp_i} \cdot \boldsymbol{v}_r^{lp_i} + m_{ls_i} \boldsymbol{a}^{ls_i} \cdot \boldsymbol{v}_r^{ls_i} +\\ &\Big((\boldsymbol{I}_{lp_i} + \boldsymbol{I}_{ls_i}) \cdot \boldsymbol{\alpha}^{Rl_i} + \boldsymbol{\Omega}^{Rl_i} \times (\boldsymbol{I}_{ls_i} + \boldsymbol{I}_{lp_i}) \boldsymbol{\Omega}^{Rl_i}\Big) \cdot \boldsymbol{\omega}_r^{Rl_i}) + m_1 \boldsymbol{g} \cdot \boldsymbol{v}_r^{cm_1} + m_2 \boldsymbol{g} \cdot \boldsymbol{v}_r^{cm_2} +\\ &m_3 \boldsymbol{g} \cdot \boldsymbol{v}_r^{cm_3} + m_4 \boldsymbol{g} \cdot \boldsymbol{v}_r^{cm_4} + m_5 \boldsymbol{g} \cdot \boldsymbol{v}_r^{cm_5} \quad r = 1,2,\dots,9\end{aligned} \tag{39}$$

And the vector X is:

$$\boldsymbol{X} = [T_1\ T_2\ F_s\ F_{l_1}\ F_{l_2}\ F_{l_3}\ F_{l_4}\ F_{l_5}\ F_{l_6}]^T \tag{40}$$

Where $F_{l_1}, \dots, F_{l_6}$ are the absolute values of forces that the $1^{st}, \dots, 6^{th}$ linear actuators apply respectively at the movable platform. T_1 and T_2 are the absolute values of the active torques applied at the 1^{st} and 2^{nd} rotation joints and F_s is the absolute value of the active force applied at the prismatic joint of the serial robot. The inverse dynamic is derived multiplying both sides of the Eq. (37) by the inverse matrix of $\boldsymbol{A}$. The inverse dynamic was simulated for a movement of the robot as it is described at Tab. 1. The result is showed at Fig. 3.

Table 1. Behavior of the generalized coordinates for simulation of the inverse dynamic

i	q_i
1	$0.03cos(0,4t)$
2	$0,02cos(0,4t+0,5)$
3	$0,5+0,035cos(0,4t)$
4	$(\pi/9)cos(0,2t+0,2)$
5	$(\pi/9)cos(0,2t+0,3)$
6	$(\pi/9)cos(0,2t+0,4)$
7	$(\pi)cos(0,5t)$
8	$(\pi/3)cos(0,5t)$
9	$(0,15)cos(0,2t+\pi/2)$

5. CONCLUSION

In this work it was proposed a novel 9 degree of freedom hybrid robotic manipulator to simulate the behavior of a crane operating on a floating platform. This hybrid manipulator is composed by a modified SCARA robot coupled to a Stewart-Gough platform. The dynamic equations of movement of this hybrid manipulator were derived. To derive these equations it was used a new approach that combines the Kane's method with the exponential formulation to represent rotations. Also, the inverse dynamic of this robot was derived and simulated.

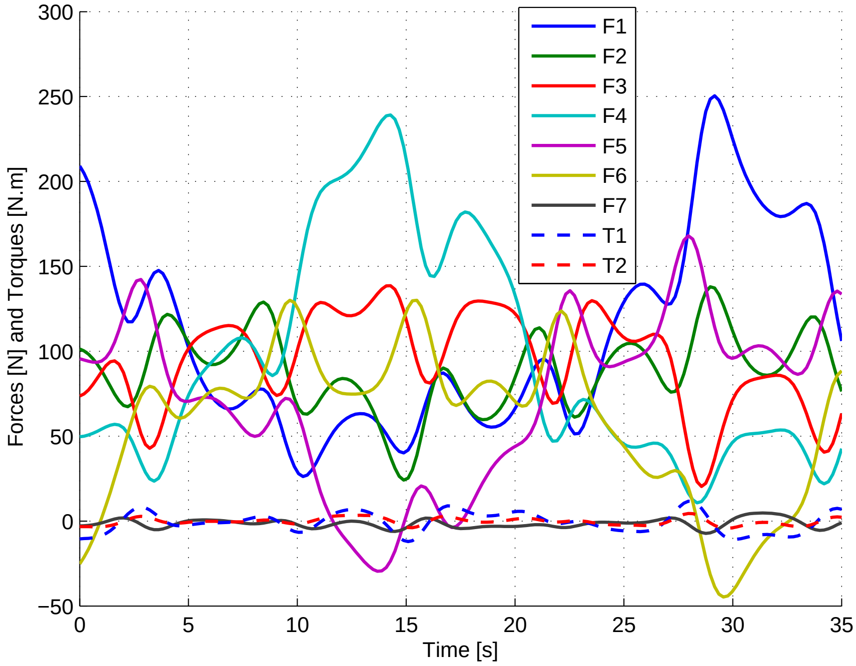

Figure 3. Active forces and torques at the hybrid robot

6. ACKNOWLEDGEMENTS

I would thank to the CNPq for the financial support.

7. REFERENCES

Alvarado, J.G., 2005. "Kinematics of a hybrid manipulator by means of screw theory". *Mulibody System Dynamics*, Vol. 14, No. 3, pp. 345–366.

Kane, T.R. and Levinson, D.A., 1985. *Dynamics, theory and applications*. McGraw Hill.

Liu, M.J., Li, C.X. and Li, C.N., 2000. "Dynamics analysis of the gough-stewart platform manipulator". *Robotics and Automation, IEEE Transactions on*, Vol. 16, No. 1, pp. 94–98.

Liu, W.F., Gong, Z.B. and Hong, Q.Q., 2005. "Investigation on kane dynamic equations based on screw theory for openchain manipui. ators". *Applied Mathematics and Mechanics*, Vol. 26, No. 5, pp. 627–635.

Meng, Q., Zhang, T., He, J.f., Song, J.y. and Han, J.w., 2010. "Dynamic modeling of a 6-degree-of-freedom stewart platform driven by a permanent magnet synchronous motor". *Journal of Zhejiang University SCIENCE C*, Vol. 11, No. 10, pp. 751–761.

Merlet, J.P., 2006. *Parallel Robots*. Springer, Netherlands, 2nd edition.

Murray, R.M., Li, Z. and Sastry, S.S., 1994. *A Mathematical Introduction to Robotic Manipulationl*. CRC Press, New Delhi, 1st edition.

Siciliano, B., Sciavicco, L., Villani, L. and Oriolo, G., 2009. *Robotics Modelling, Planning and Control*. Springer, London, 1st edition.

Tanev, T.K., 2000. "Kinematics of a hybrid (parallel-serial) robot manipulator". *Mechanism and Machine Theory*, Vol. 35, No. 9, pp. 1183–1196.

Wu, P., Xiong, H. and Kong, J., 2012. "Dynamic analysis of 6-sps parallel mechanism". *International Journal of Mechanics and Materials in Design*, Vol. 8, No. 2, pp. 121–128.

Yang, C., Han, J., Zheng, S. and Peter, O.O., 2012. "Dynamic modeling and computational efficiency analysis for a spatial 6-dof parallel motion system". *Nonlinear Dynamics*, Vol. 67, No. 2, pp. 1007–1022.

8. RESPONSIBILITY NOTICE

The authors are the only responsible for the printed material included in this paper.